### Title
Limiting Current Density in Single-Ion-Conducting and Conventional Block Copolymer Electrolytes




### Journal
Journal of The Electrochemical Society, 169(4)

### ISSN
0013-4651



### Authors
Hoffman, Zach J
Ho, Alec S
Chakraborty, Saheli
et al.



### Publication Date
2022-04-01

### DOI
10.1149/1945-7111/ac613b

Peer reviewed

Journal of The Electrochemical Society



OPEN ACCESS

# Limiting Current Density in Single-Ion-Conducting and Conventional Block Copolymer Electrolytes

To cite this article: Zach J. Hoffman *et al* 2022 *J. Electrochem. Soc.* **169** 043502

*Journal of The Electrochemical Society*, 2022 **169** 043502

# Limiting Current Density in Single-Ion-Conducting and Conventional Block Copolymer Electrolytes

**Zach J. Hoffman,[1,2,3] Alec S. Ho,[1,2] Saheli Chakraborty,[1,2,4] and Nitash P. Balsara[1,2,3,4,z]**

[1]*Department of Chemical and Biomolecular Engineering, University of California, Berkeley, Berkeley, California 94720, United States of America*
[2]*Materials Sciences Division, Lawrence Berkeley National Laboratory, Berkeley, California 94720, United States of America*
[3]*Joint Center for Energy Storage Research (JCESR), Lawrence Berkeley National Laboratory, Berkeley, California 94720, United States of America*
[4]*Energy Storage and Distributed Resources Division, Lawrence Berkeley National Laboratory, Berkeley, California 94720, United States of America*

The limiting current density of a conventional polymer electrolyte (PS-PEO/LiTFSI) and a single-ion-conducting polymer electrolyte (PSLiTFSI-PEO) was measured using a new approach based on the fitted slopes of the potential obtained from lithium-polymer-lithium symmetric cells at a constant current density. The results of this method were consistent with those of an alternative framework for identifying the limiting current density taken from the literature. We found the limiting current density of the conventional electrolyte is inversely proportional to electrolyte thickness as expected from theory. The limiting current density of the single-ion-conducting electrolyte was found to be independent of thickness. There are no theories that address the dependence of the limiting current density on thickness for single-ion-conducting electrolytes.
 [DOI: 10.1149/1945-7111/ac613b]

Manuscript submitted December 15, 2021; revised manuscript received February 7, 2022. Published April 4, 2022.

Supplementary material for this article is available online

## List of symbols

| | |
|---|---|
| $C_b$ | salt concentration (mol cm$^{-3}$) |
| $D$ | salt diffusion coefficient (cm$^2$ s$^{-1}$) |
| $F$ | Faraday's constant (C mol$^{-1}$) |
| $i$ | applied current density (mA cm$^{-2}$) |
| $i_L$ | limiting current density (mA cm$^{-2}$) |
| $L$ | electrolyte thickness ($\mu$m) |
| LiTFSI | lithium bis(trifluoromethanesulfonyl)imide |
| PS-PEO | polystyrene–*b*–polyethylene oxide |
| PSLiTFSI-PEO | polystyrene-LiTFSI–*b*–polyethylene oxide |
| $r$ | molar ratio of lithium ions to ethylene oxide units (r = [Li$^+$]/[EO]) |
| $t_+$ | cationic transference number |
| t | measurement time (hr) |
| **Greek** | |
| $\kappa$ | conductivity (S/cm) |
| $\Phi$ | potential (mV) |
| $\Phi_0$ | initial potential (mV) |
| $\rho_+$ | current fraction |

Lithium-ion batteries are common energy sources for many applications, and as their use grows there is increasing interest in developing the next generation of rechargeable batteries.[1–3] Conventional lithium-ion batteries utilize a liquid electrolyte that is a mixture of organic solvents and a lithium salt. These electrolytes are highly flammable and this contributes to safety concerns.[4] A potential solution to resolve this issue is the use of polymer electrolytes which have reduced flammability.[5,6] Polymer electrolytes, particularly block copolymer electrolytes, are also of interest because of their chemical stability against lithium metal anodes.[5,7–11] Polymer electrolytes are generally prepared by mixing a lithium salt into the polymer.

The adoption of polymer electrolytes is dependent on their electrochemical performance and the limits under which they can operate. When current is passed through polymer electrolytes, salt accumulates near the anode and is depleted near the cathode. In this respect, polymer electrolytes are no different from conventional liquid electrolytes; these systems are referred to as binary electrolytes. The largest sustainable current density that can be passed through the electrolyte is known as the limiting current density.[12–15] At this value of current density the concentration of lithium salt at the cathode is zero, and operating at current densities above this value results in cell failure.[14] Measurements of the limiting current density of electrolytes are uncommon, with few historical examples in the literature.[16–18] However, there have been several recent reports of measurements of the limiting current density in polymer electrolytes.[10,19–23]

Newman derived a simple expression for the limiting current density of an electrolyte of thickness $L$ placed between two planar electrodes:

$$i_L = \frac{2C_bDF}{(1 - t_+)L}, \qquad [1]$$

where $i_L$ is the limiting current, $C_b$ is the salt concentration, $D$ is the salt diffusion coefficient, $F$ is Faraday's constant, $t_+$ is the cationic transference number, and $L$ is the thickness of the electrolyte.[14] This equation applies to mixtures of salts and a solvent (either a liquid or a polymer) wherein the transport coefficients are independent of salt concentration. Note that the limiting current density is inversely proportional to $L$.

Single-ion-conducting polymer electrolytes are systems wherein the anions are covalently bound to the polymer chain; the unbound counterions (cations) are, in principle, free to move. If we neglect chain mobility, then the only mobile species are the counterions. There are no liquid analogs of single-ion-conducting polymer electrolytes. However, all inorganic ceramic and glass electrolytes are single-ion-conductors.[24] Concentration gradients cannot develop in these systems without disrupting charge neutrality across the electrolyte.[14,25] In the absence of concentration gradients, the lithium salt concentration cannot reach zero at the cathode, and traditional approaches for defining limiting current density fail. It is also worth noting that as $t_+ \to 1$, Eq. 1 predicts that $i_L \to \infty$.

To our knowledge, the dependence of limiting current density on electrolyte thickness has not been measured in either binary

[z]E-mail: nbalsara@berkeley.edu

electrolytes or single-ion-conducting electrolytes. It is convenient to quantify limiting current density in a lithium-electrolyte-lithium cell as the distance between the electrodes is well-defined. It is well known that the passage of high current densities results in the formation of dendrites at lithium metal anodes,[26–28] and this complicates determination of limiting current density. Dendrite growth is suppressed in block copolymer electrolytes due to their high elastic modulus.[29,30] We therefore use a block copolymer (polystyrene–*b*–polyethylene oxide (PS-PEO)) with added lithium bis(trifluoromethanesulfonyl)imide (LiTFSI) salt to experimentally determine the relationship between limiting current density and electrolyte thickness in binary electrolytes. For consistency, our single-ion-conductor is also a block copolymer (polystyrene–LiTFSI–*b*–polyethylene oxide (PSLiTFSI-PEO)). Our main goal is to contrast the thickness dependence of the limiting current density in these two systems. This required the development of a new framework for quantifying limiting current density in single-ion-conducting systems. We show that the same framework also applies to the conventional binary polymer electrolyte.

## Experimental

***Polymer synthesis.—***For this study two polymers were used, polystyrene–*b*–polyethylene oxide (PS-PEO) and polystyrene–LiTFSI–*b*–polyethylene oxide (PSLiTFSI-PEO). The synthesis of both these polymers is well documented in the literature.[31,32] For PS-PEO the molecular weight of the polystyrene and polyethylene oxide blocks are 200 and 222 kg mol$^{-1}$ respectively. With PSLiTFSI-PEO the molecular weight of the polystyrene–LiTFSI and polyethylene oxide blocks are 2.1 and 5 kg mol$^{-1}$ respectively.

***Preparation of electrolytes.—***For this study we define salt concentration $r$ as the molar ratio of LiTFSI to ethylene oxide units. The $r$ value of the PS-PEO/LiTFSI and PSLiTFSI-PEO electrolytes were 0.085 and 0.059 respectively. PS-PEO/LiTFSI electrolytes were prepared by adding LiTFSI salt to PS-PEO polymer according to the procedures outlined by Maslyn et al.[21]

***Electrochemical characterization and limiting current density measurements.—***The current fraction, $\rho_+$, of the PSLiTFSI-PEO electrolyte was found to be 0.96 ± 0.01 following procedures reported previously.[33] Strictly speaking, a single-ion-conductor would exhibit $\rho_+ = t_+ = 1.0$. It is clear that to a good approximation, the PSLiTFSI-PEO polymer is a single-ion-conductor.

Limiting current density measurements for PS-PEO/LiTFSI electrolytes were performed according to procedures outlined by Maslyn et al.[21] After an initial impedance measurement, a constant current was applied while measuring the potential, and after allowing the cell to relax another impedance measurement was made. The two impedance measurements ensure that the passage of current did not result in irreversible changes in either the bulk or interfacial impedances. The limiting current density was determined by systematically increasing the applied current density and noting the nature of the cell potential vs time data. The data presented in this paper is entirely consistent with previously published comprehensive studies on the limiting current density of PS-PEO/LiTFSI electrolytes.[21,34] We thus only made one cell at each electrolyte thickness.

For PSLiTFSI-PEO, limiting current density cells were made using lithium symmetric cells with silicone spacer material (McMaster-Carr) with thicknesses of 300, 400, 550, and 840 $\mu$m according to the procedures outlined in Ref. 33. The standard deviation of these electrolyte thicknesses is below 10% of the total thickness. These measurements were made during construction of the cells inside the glovebox, using methods described in Ref. 33. The PS-PEO/LiTFSI electrolytes were molded to give free-standing films. The thicknesses of the PSLiTFSI-PEO cells were much larger because the polymer could not be processed to give free-standing films. The limiting current density experiments were performed after being preconditioned with ±0.02 mA cm$^{-2}$, following Ref. 33. After preconditioning, the cells were subjected to various current densities while measuring the resulting potential. For the PSLiTFSI-PEO electrolytes, three to six cells were used for each measurement.

***X-ray microtomography.—***After experimentation, these pouch cells with PS-PEO/LiTFSI electrolytes were opened inside a glovebox, and a portion of the symmetric cell was cut out and repouched. The repouched cells were imaged using hard X-ray microtomography at Beamline 8.3.2 at the Advanced Light Source at Lawrence Berkeley National Laboratory, following the procedures of Ref. 21. Cells were imaged at 4 × magnification, corresponding to a pixel size of approximately 1.625 $\mu$m. The attenuation-based tomograms were reconstructed using TomoPy.[35] Electrolyte thickness, $L$, corresponds to the average distance between approximately parallel electrodes and was determined by measuring at least 10 points within the cell using the software ImageJ on tomographic cross-sections of each cell. The PS-PEO/LiTFSI films in this study had thicknesses of 33.5, 53.0, 67.7, and 74.3 $\mu$m. The standard deviation of each thickness measurement ranged from 2%–6% of the total thickness.

## Results and Discussion

Limiting current density is measured in experiments where a steady current density is drawn across a lithium-electrolyte-lithium symmetric cell and the potential drop across the cell is measured as a function of time. Typical data obtained from the PS-PEO/LiTFSI electrolyte are shown in Fig. 1a, where $\Phi/L$ is plotted as a function of time for an average electrolyte thickness, $L$, of 53.0 $\mu$m. $\Phi$ represents the potential drop across the electrolyte after correcting for the potential drop across the electrolyte-electrode interfaces as described in Ref. 19. This correction, which is the product of the applied current and interfacial resistance of the electrolyte, ranges from 10%–40% of the total measured potential for PSLiTFSI-PEO and 30%–50% for PS-PEO/LiTFSI. Characteristic impedance data for both electrolytes can be found in the supplementary material (available online at stacks.iop.org/JES/169/043502/mmedia). In this work we plot $\Phi/L$ to remove the potential drop due to interfacial resistances, and so that cells of different thicknesses can be compared on the same scale; the limiting current density of an electrolyte is a bulk property and thus removing interfacial effects is necessary. When the applied current density is below the limiting current density, the potential reaches a steady state value at long times; the data obtained at current densities well below the limiting current density are shown in the inset of Fig. 1a. When current densities above the limiting current density are applied, the potential never stabilizes and at high enough current densities, the potential increases exponentially. Responses below and above the limiting current density are shown in Fig. 1a. The time dependence of $\Phi/L$ reflects the formation of salt concentration gradients under the applied current.

Figure 1b shows a series of $\Phi/L$ vs time plots, when a steady current density is drawn across a symmetric cell with PSLiTFSI-PEO electrolyte, with $L$ of 400 $\mu$m. The applied current densities in this experiment are about an order of magnitude lower than those given in Fig. 1a. The main reason for this is the difference in electrolyte thicknesses; the product $iL$ is similar for both electrolyte types discussed in this work. At low current densities, the potential is independent of time. This constant potential is unsurprising as no concentration gradients are expected to develop in single-ion-conducting electrolytes. As larger values of current density are applied, the potential increases with time. This increase is most clear at $i = 0.4$ mA cm$^{-2}$, the highest current density used in this series of experiments. The $\Phi/L$ vs time behaviors at low and high current densities in a block copolymer with added salt and a single-ion conductor differ qualitatively as shown in Fig. 1. Thus, analyzing these data sets in a consistent manner to determine the limiting current density is non-trivial.

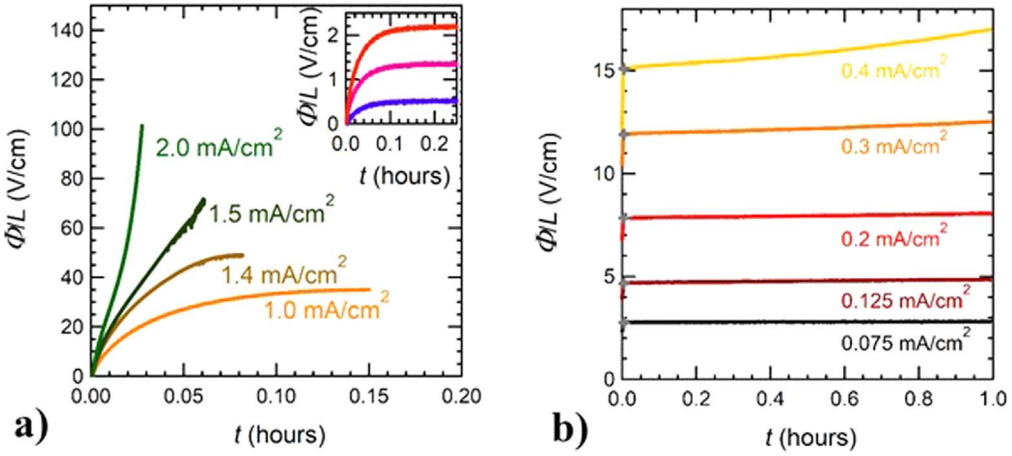


**Figure 1.** Electric potential response to various applied current densities for the (a) PS-PEO/LiTFSI electrolyte and (b) PSLiTFSI-PEO electrolyte plotted as a function of time. Φ, the electric potential, is normalized by electrolyte thickness, *L*. Inset of (a) shows potential responses at current densities of 0.02, 0.05, and 0.08 mA $cm^{-2}$.

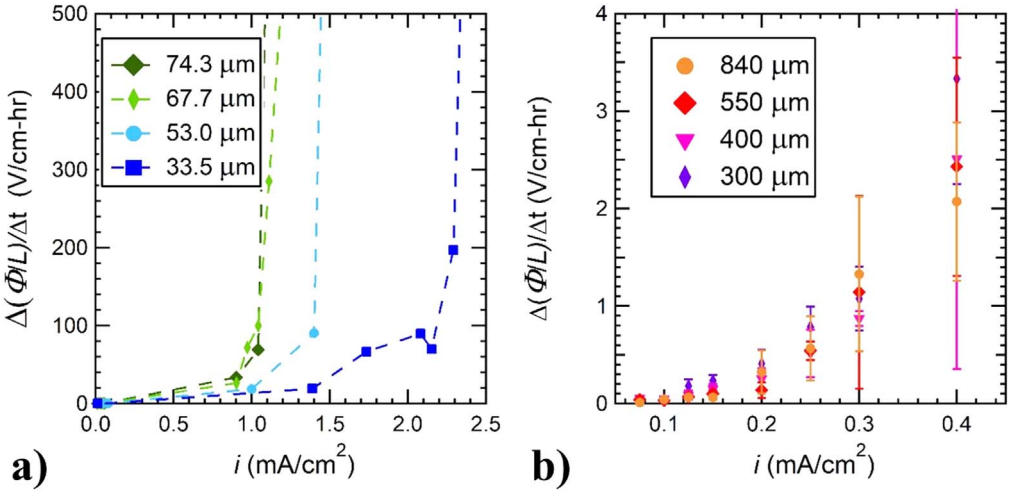


**Figure 2.** Plots of the fitted slopes, $\Delta(\Phi/L)/\Delta t$, obtained from final 20% of measurement time as a function of applied current density, *i*, for the (a) PS-PEO/LiTFSI electrolyte and (b) PS LiTFSI-PEO electrolyte.

Our analysis method focuses on the time dependence of $\Phi/L$ during the final 20% of the measurement time ($\Delta t$). When the limiting current density is exceeded in a binary electrolyte, the potential shoots up toward the end of the experiment. In contrast, when the applied current density is below the limiting current, the potential approaches a time-independent constant plateau. The distinction between these two regimes can readily be seen when the long-time behavior is examined. For consistency we use the final 20% of the measurement time to analyze both the conventional polymer electrolytes and the single-ion-conducting electrolytes. We fit the $\Phi/L$ vs time data in this regime to linear functions and examine the slopes.

Figures 2a and 2b show the results of our analysis. Here we plot the slopes, $\Delta(\Phi/L)/\Delta t$, vs the applied current density, *i*. Figure 2a shows data obtained from PS-PEO/LiTFSI electrolytes. It can be clearly seen for each thickness that at low current densities $\Delta(\Phi/L)/\Delta t$ changes minimally with increasing current, until a threshold is reached. For $L = 74.3\ \mu m$, the threshold is in the vicinity of $i = 1.0$ mA $cm^{-2}$, while for $L = 33.5\ \mu m$, the threshold is in the vicinity of $i = 2.4$ mA $cm^{-2}$. It is clear that the threshold is thickness-dependent for PS-PEO/LiTFSI electrolytes. This analysis was repeated for four different thicknesses of PSLiTFSI-PEO electrolytes, and the results are shown in Fig. 2b. The data in Fig. 2b also exhibit two regimes, wherein $\Delta(\Phi/L)/\Delta t$ changes minimally with increasing current density until a threshold is reached in the vicinity of $i = 2.3$ mA $cm^{-2}$. However, there is a modest change in $\Delta(\Phi/L)/\Delta t$ when this threshold is crossed. More importantly, changing the electrolyte thickness from 300 to 840 $\mu$m has no effect on the threshold current. In Fig. 2b, the error bars reflect the standard deviation of the obtained values.

We posit that the value of current density at which the slope $\Delta(\Phi/L)/\Delta t$ begins to increase rapidly is indicative of the limiting current density of that electrolyte. To quantify the actual value of the limiting current, each data set in Figs. 2a and 2b was separated into two regimes, and data within each regime were fit to a straight line. The demarcation between the two regimes (current density) was systematically changed to minimize the sum of squared error. The point of intersection of the two-lines fit was defined as the limiting current.

The distinction between the two regimes was much clearer in the PS-PEO/LiTFSI electrolytes, and this led to unambiguous determination of the limiting current. Example fits obtained for the thinnest and thickest PS-PEO/LiTFSI electrolytes are shown in Fig. 3a. In these electrolytes, following Ref. 20, one could also determine limiting current density by averaging the highest sustainable current, where a steady potential is reached, and the lowest unsustainable current, where no steady state is reached. We refer to this approach as the conventional approach. This value is shown by arrows in

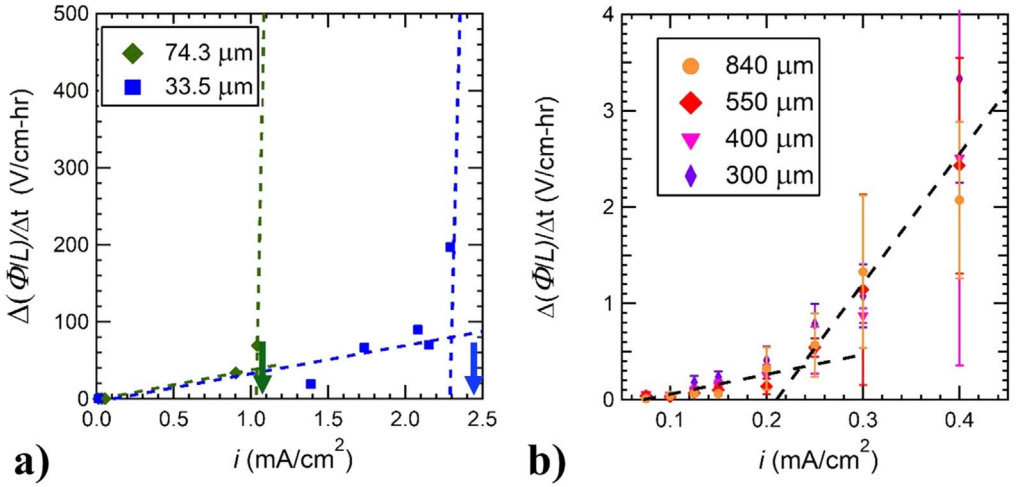


**Figure 3.** linear fits of data from Fig. 2 used to determine limiting current. (a) Two-line fits through data obtained from PS-PEO/LiTFSI electrolytes with the largest and smallest thicknesses. Arrows indicate the value of limiting current density determined by the approach from Ref. 20 for PS-PEO/LiTFSI. (b) Two-line fit through the data obtained from PSLiTFSI-PEO electrolytes. The data obtained from all four electrolyte thicknesses are consistent with the fit shown.

Fig. 3a. It is clear that both approaches give consistent estimates of the limiting current density. The result of our fitting procedure for PSLiTFSI-PEO is shown in Fig. 3b. We conclude from this analysis that the limiting current density of PSLiTFSI-PEO is 0.235 mA $cm^{-2}$, and it is the same for all four thicknesses.

In Fig. 4 we plot the limiting current density ($i_L$) as a function of $1/L$, where the top axis corresponds to PS-PEO/LiTFSI and the bottom corresponds to PSLiTFSI-PEO. Figure 4 contains the results of both the conventional method for determining limiting current density in PS-PEO/LiTFSI (purple circles) along with the slopes method proposed in this work (pink circles). For PS-PEO/LiTFSI, the horizontal error bars reflect the standard deviations of $L$ recorded from a given cell, using X-ray microtomography as described in the experimental section. For the conventional method, $i_L$ was plotted as the midpoint of the largest sustainable current density and the smallest unsustainable current. The vertical error bars represent these bounds.

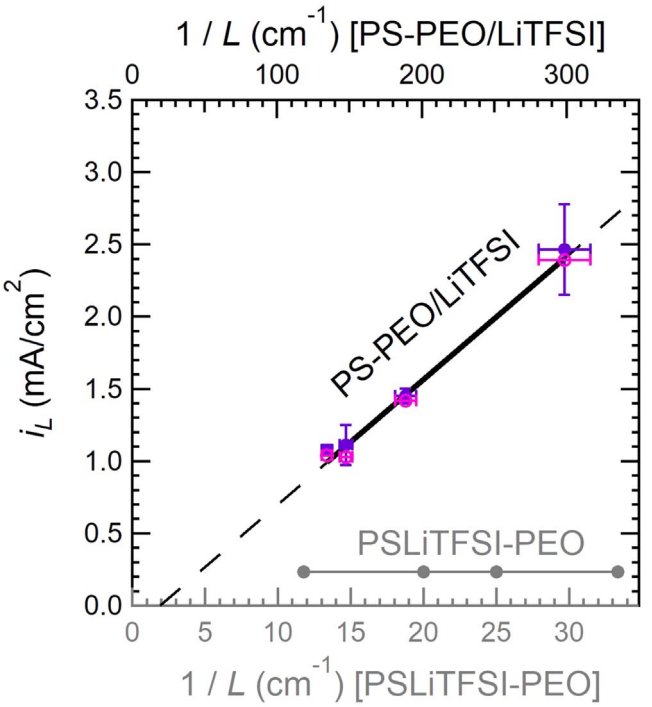


**Figure 4.** Limiting current density plotted as a function of $1/L$, where $L$ is the electrolyte thickness. The top axis is for PS-PEO/LiTFSI, and the bottom axis is for PSLiTFSI-PEO. The two different $x$-axes are required because the average thicknesses of the electrolytes used in the symmetric cell experiments on the two systems were different. Dark purple data points correspond to the limiting current density determined using the conventional method, and the pink circles correspond to the limiting current density determined using the slopes method.

As seen in Fig. 4, the limiting current density of PS-PEO/LiTFSI is a linear function of $1/L$. Extrapolation of the linear fit through all 8 data points gives an intercept that is very close to zero. Both facts are consistent with Eq. 1, indicating that our data are consistent with the conventional definition of limiting current density, defined as the current density at which the LiTFSI concentration at the negative electrode approaches zero. Electrolyte failure occurs when the limiting current density is exceeded; the rapid increase in cell potential is due to irreversible reactions between the electrode and the LiTFSI-free electrolyte. However, the fact that the limiting current density of PSLiTFSI-PEO is independent of electrolyte thickness indicates that electrolyte failure must occur due to some other reason. We posit that beyond the limiting current density the cell potential increases more steeply than expected due to irreversible reactions between the electrode and the single-ion-conducting electrolyte. Which portion of the polymer chain participates in these reactions (charged or neutral moieties) remains an open question.

The limiting current density of PSLiTFSI-PEO is independent of electrolyte thickness over the range of thicknesses covered in this work. This is a novel result that has not been reported in the literature. This independence with respect to thickness is further indication of the lack of concentration gradients within this electrolyte. Further studies are required to directly identify the physical underpinnings of this result.

We conclude this section by reexamining the voltage vs time curves obtained from the single-ion-conducting electrolyte, PSLiTFSI-PEO, shown in Fig. 1b. Our analysis thus far has focused on the behavior at long times, the final 20% of our time window. For completeness, in Fig. 5 we examine the initial potential, $\Phi_0/L$, obtained after the potentiostat has stabilized. These values are marked by crosses in Fig. 1b. In separate experiments this electrolyte was studied in symmetric cells using AC impedance and the conductivity, $\kappa$, thus obtained was $2.85 \times 10^{-5} \pm 4.78 \times 10^{-6}$ S $cm^{-1}$. A single-ion conductor must obey Ohm's law,

$$\kappa = i\left(\frac{L}{\Delta V}\right), \qquad [2]$$

due to the absence of concentration polarization at all values of applied current.[36] The line in Fig. 5 has a slope $1/\kappa$. The error bars in

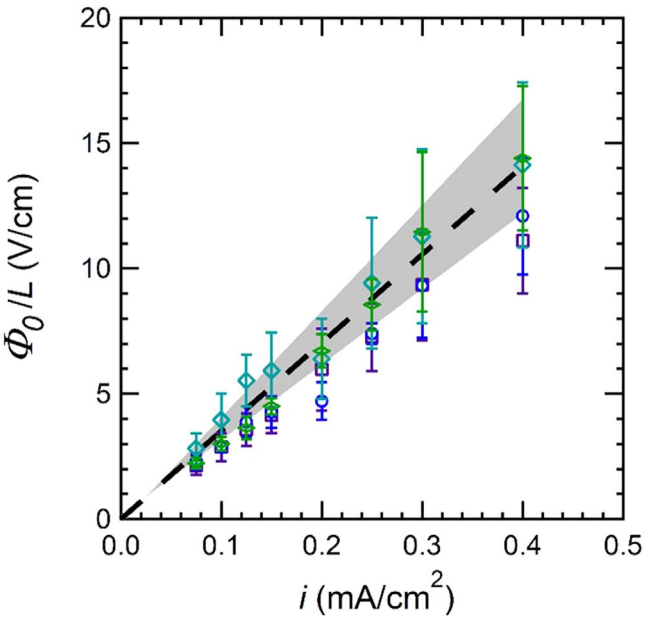


**Figure 5.** Initial values of the normalized potential, $\Phi_0/L$, as a function of applied current for PSLiTFSI-PEO. Each symbol represents the thickness of the electrolyte, $L$. ( = 300 $\mu$m, = 400 $\mu$m, = 550 $\mu$m, = 840 $\mu$m). The dashed black line has a slope $1/\kappa$, and error in conductivity is shown by the gray shading.

Fig. 5 represent the standard deviation of the initial potential for each thickness at the corresponding applied currents. The experimentally measured values of $\Phi_0$ are in reasonable agreement with expectations, irrespective of whether the applied current density was above or below the limiting current.

## Conclusions

We have examined the time dependence of potential obtained from lithium-polymer-lithium symmetric cells at constant current density. We have shown that for a conventional polymer electrolyte (PS-PEO/LiTFSI), the limiting current density is proportional to the inverse of the electrolyte thickness. While this behavior is expected and consistent with theory, we were unable to find any other studies of the effect of electrolyte thickness on limiting current density in the literature. We propose a new approach for consistently determining limiting current density in both conventional electrolytes and single-ion-conducting electrolytes. The measured limiting current density of a single-ion-conducting electrolyte (PSLiTFSI-PEO) was found to be independent of electrolyte thickness. This phenomenon has not been documented before in the literature. It has interesting implications for developing electrolytes to increase the lifetime of rechargeable batteries, as increasing electrolyte thickness has no effect on the window of current densities that can be drawn across the electrolyte. Further studies are needed to better understand what causes this failure within the PSLiTFSI electrolytes, and to determine if our framework can be used to determine the limiting current density of other single-ion-conductors such as inorganic crystals and glasses.

## Acknowledgments

This work was intellectually led by the Joint Center for Energy Storage Research (JCESR), an Energy Innovation Hub funded by the U.S. Department of Energy, Office of Science, Office of Basic Energy Science, under Contract No. DE-AC02–06CH11357, which supported characterization work conducted by Z. J. H. under the supervision of N.P.B. A.S.H was supported by a National Science Foundation Graduate Research Fellowship DGE-2020294884. The authors thank Kevin Gao and Louise Frenck for useful discussion related to this work.

## ORCID

Zach J. Hoffman https://orcid.org/0000-0002-8989-8077
Alec S. Ho https://orcid.org/0000-0003-1373-5332
Nitash P. Balsara https://orcid.org/0000-0002-0106-5565

## References

1. L. Trahey et al., *Proc. Natl. Acad. Sci. U. S. A.*, **117**, 12550 (2020).
2. X. Q. Zhang, C. Z. Zhao, J. Q. Huang, and Q. Zhang, *Engineering*, **4**, 831 (2018).
3. Q. Wang, L. Jiang, Y. Yu, and J. Sun, *Nano Energy*, **55**, 93 (2019).
4. C. Arbizzani, G. Gabrielli, and M. Mastragostino, *J. Power Sources*, **196**, 4801 (2011).
5. D. T. Hallinan and N. P. Balsara, *Annu. Rev. Mater. Res.*, **43**, 503 (2013).
6. K. S. Ngai, S. Ramesh, K. Ramesh, and J. C. Juan, *Ionics (Kiel).*, **22**, 1259 (2016).
7. A. S. Ho, P. Barai, J. A. Maslyn, L. Frenck, W. S. Loo, D. Y. Parkinson, V. Srinivasan, and N. P. Balsara, *ACS Appl. Energy Mater.*, **3**, 9645 (2020).
8. L. Frenck, G. K. Sethi, J. A. Maslyn, and N. P. Balsara, *Front. Energy Res.*, **0**, 115 (2019).
9. L. Frenck, V. D. Veeraraghavan, J. A. Maslyn, A. Müller, A. S. Ho, W. S. Loo, A. M. Minor, and N. P. Balsara, *Solid State Ionics*, **358**, 115517 (2020).
10. G. K. Sethi, L. Frenck, S. Sawhney, S. Chakraborty, I. Villaluenga, and N. P. Balsara, *Solid State Ionics*, **368**, 115702 (2021).
11. V. D. Veeraraghavan, L. Frenck, J. A. Maslyn, W. S. Loo, D. Y. Parkinson, and N. P. Balsara, *ACS Appl. Mater. Interfaces*, **13**, 27006 (2021).
12. E. A. Hogge and M. B. Kraichman, *J. Am. Chem. Soc.*, **76**, 1431 (1954).
13. J. Newman, *J. Electrochem. Soc.*, **113**, 1235 (1966).
14. J. Newman and K. E. Thomas-Alyea, *Electrochemical Systems* (Wiley, New Jersey, NJ) 3rd ed. (2004).
15. H. S. Sand, *Proc. Phys. Soc. London*, **17**, 496 (1899).
16. C. O. Laoire, E. Plichta, M. Hendrickson, S. Mukerjee, and K. M. Abraham, *Electrochim. Acta*, **54**, 6560 (2009).
17. J. W. Park, K. Yoshida, N. Tachikawa, K. Dokko, and M. Watanabe, *J. Power Sources*, **196**, 2264 (2011).
18. S. I. Lee, U. H. Jung, Y. S. Kim, M. H. Kim, D. J. Ahn, and H. S. Chun, *Korean J. Chem. Eng.*, **19**, 638 (2002).
19. D. A. Gribble, L. Frenck, D. B. Shah, J. A. Maslyn, W. S. Loo, K. I. S. Mongcopa, D. M. Pesko, and N. P. Balsara, *J. Electrochem. Soc.*, **166**, A3228 (2019).
20. D. B. Shah, H. K. Kim, H. Q. Nguyen, V. Srinivasan, and N. P. Balsara, *J. Phys. Chem. C*, **123**, 23872 (2019).
21. J. A. Maslyn, L. Frenck, V. D. Veeraraghavan, A. Müller, A. S. Ho, N. Marwaha, W. S. Loo, D. Y. Parkinson, A. M. Minor, and N. P. Balsara, *Macromolecules*, **54**, 4010 (2021).
22. H. O. Ford, B. Park, J. Jiang, M. E. Seidler, and J. L. Schaefer, *ACS Mater. Lett.*, **2**, 272 (2020).
23. Z. Chen, D. Steinle, H. D. Nguyen, J. K. Kim, A. Mayer, J. Shi, E. Paillard, C. Iojoiu, S. Passerini, and D. Bresser, *Nano Energy*, **77**, 105129 (2020).
24. D. J. Siegel, L. Nazar, Y. M. Chiang, C. Fang, and N. P. Balsara, *Trends Chem.*, **3**, 807 (2021).
25. M. Doyle, T. Fuller, and J. Newman, *Electrochim. Acta1*, **39**, 2073 (1993).
26. R. Selim and P. Bro, *J. Electrochem. Soc.*, **121**, 1457 (1974).
27. I. Epelboin, M. Froment, M. Garreau, J. Thevenin, and D. Warin, *J. Electrochem. Soc.*, **127**, 2100 (1980).
28. D. Lin, Y. Liu, and Y. Cui, *Nat. Nanotechnol. 2017 123*, **12**, 194 (2017).
29. C. Monroe and J. Newman, *J. Electrochem. Soc.*, **150**, A1377 (2003).
30. C. Monroe and J. Newman, *J. Electrochem. Soc.*, **152**, A396 (2005).
31. A. A. Rojas, (2017), Single-Ion-Conducting Block Copolymer Electrolytes for Lithium Batteries: Morphology, Ion Transport, and Mechanical Properties. *UC Berkeley*. https://escholarship.org/uc/item/4572w66m.
32. N. Hadjichristidis, H. Iatrou, S. Pispas, and M. Pitsikalis, *J. Polym. Sci., Part A: Polym. Chem.*, **38**, 3211 (2000).
33. Z. J. Hoffman, D. B. Shah, and N. P. Balsara, *Solid State Ionics*, **370**, 115751 (2021).
34. L. Frenck, V. D. Veeraraghavan, J. A. Maslyn, and N. P. Balsara, *Electrochim. Acta*, **409**, 139911 (2022).
35. D. Gürsoy, F. De Carlo, X. Xiao, and C. Jacobsen, *J. Synchrotron Radiat.*, **21**, 1188 (2014).
36. M. D. Galluzzo, J. A. Maslyn, D. B. Shah, and N. P. Balsara, *J. Chem. Phys.*, **151**, 020901 (2019).